Improving the Performance of Coded FDFR Multi-Antenna Systems with Turbo-Decoding

Renqiu Wang[1]*, Xiaoli Ma*[2] *and Georgios B. Giannakis*[1]

[1]Dept. of ECE., Univ. of Minnesota, Minneapolis MN 55455, USA
[2]Dept. of ECE., Auburn University, Auburn AL 36849, USA

Abstract — A full-diversity full-rate (FDFR) design was developed recently, to enable an uncoded layered space-time (LST) system to achieve full-diversity (N_tN_r) and full-rate (N_t symbols per channel use) simultaneously, for any number of transmit antennas N_t and receive antennas N_r. In this paper, we investigate the performance of a coded FDFR system obtained by concatenating an error control coding (ECC) module and an FDFR module with a random interleaver in between. Iterative decoding is performed at the receiver. With R_c denoting the ECC rate, and d the minimum Hamming distance, an overall transfer rate of R_cN_t symbols per channel use and a full diversity order dN_tN_r are achieved. Compared with coded V-BLAST, without sacrificing rate the coded FDFR system offers evident performance improvement when relatively weak codes are used. As N_r increases, even such a strong code as rate 1/2 turbo codes can benefit from FDFR. Specifically, 1.5dB gain over coded V-BLAST is obtained in a 2×2 antenna setup when convolutional codes or rate 3/4 turbo codes are used. 0.5dB gain is offered in a 2×5 setup when rate 1/2 turbo code is used. The price paid is increased complexity.

Keywords: space-time, high rate, diversity, V-BLAST, FDFR

I. Introduction

High rate and high performance are the ultimate goals of modern wireless communications. These are challenged by multiplicative channel fading and additive Gaussian noise effects. Traditional error control coding (ECC) over the Galois field (GF) cope with the noise and fading by adding redundancy, and thus sacrificing spectral efficiency; while other efforts aim to mitigate the channel fading by exploiting diversity flavors in other dimensions. Linear complex field (LCF) coding and space-time (ST) coding are two such flavors, in the modulation and spatial dimensions, respectively. By concatenating an LCF coder and an LST mapper properly, the recently developed full-diversity full rate (FDFR) design [1] enables an *uncoded* layered ST (LST) system to have full diversity (N_tN_r) and full-rate (N_t symbols per channel use) simultaneously, where N_t and N_r denote the number of transmit and of receive antennas, respectively. Joint consideration of ECC and LCF coding (LCFC) in ST setups was pursued also in [2]. Although the triangular ST mapper developed in [2] enables full diversity order dN_tN_r, where d is the minimum Hamming distance or free distance of ECC, the overall transfer rate is only about half of the maximum possible.

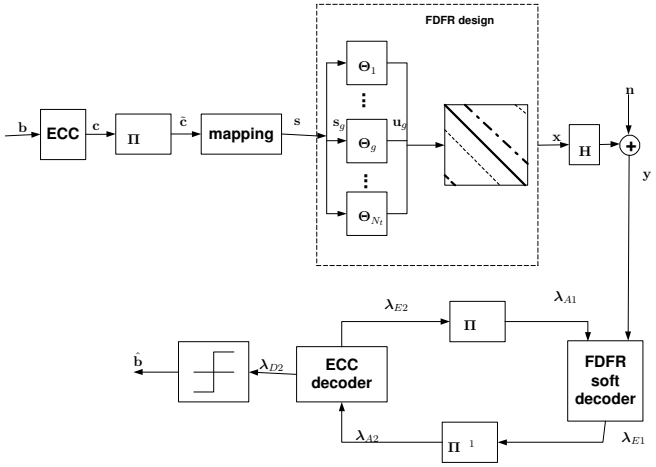

Fig. 1. the coded FDFR system model

The performance of uncoded FDFR and [2] motivate us to investigate the performance of a joint ECC and FDFR system in this paper. We will particularly consider relatively "weakly" coded FDFR architectures, which rely on the concatenation of ECC, LCFC and ST multiplexing at the transmitter, and soft-to-hard sphere decoding (SHD-SD) [3] with iterative detection at the receiver. This consideration is meaningful since under practical complexity and delay constrains, those capacity-approaching ECC's such as rate 1/2 turbo codes (TC) with large interleaver size [3, 4], or LDPC codes with large block size, can not be used. Other alternatives such as convolutional codes (CC) have to be considered. Another option is a high rate ECC (e.g., a rate 3/4 TC) that could be used at the transmitter to meet high data rate demands. In both cases, we will show by simulations that the FDFR design offers notable performance improvement by enabling full spatial diversity without sacrificing rate.

II. System model

The coded FDFR system model is depicted in Figure 1. The information bits $\mathbf{b}$ are first encoded by an ECC module to yield $\mathbf{c}$, and then go through a random interleaver Π. Interleaved bits $\tilde{\mathbf{c}}$ are mapped to symbols $\mathbf{s}$ adhering to a certain constellation; $\mathbf{s}$ is then fed to the FDFR module to output N_t^2 symbols per

FDFR coded block. Each FDFR block is divided into N_t sub-blocks with sub-block length equal to N_t. Let $\mathbf{s}_g$ denote the gth $N_t \times 1$ sub-block ($g = 1, \ldots, N_t$), whose entries $\{s_{g,k}\}_{k=1}^{N_t}$ are drawn from a complex finite alphabet $\mathcal{S}$. The sub-block $\mathbf{s}_g$ is first coded to obtain

$$\mathbf{u}_g = \mathbf{\Theta}_g \mathbf{s}_g, \quad g = 1, \ldots, N_t, \tag{1}$$

where $\mathbf{\Theta}_g := \beta^{g-1}\mathbf{\Theta}$ is the LCF encoders, β is a scalar, and $\mathbf{\Theta}$ is chosen from the class of unitary Vandermonde matrices:

$$\mathbf{\Theta} = \frac{1}{\sqrt{N_t}} \mathbf{F}_{N_t}^{*} \mathrm{diag}[1, \alpha, \ldots, \alpha^{N_t-1}], \tag{2}$$

where $\mathbf{F}_{N_t}$ is the $N_t \times N_t$ FFT matrix with $(m+1, n+1)$st entry $e^{-j2\pi mn/N_t}$, * denotes Hermitian transposition, and α is a scalar. Three design approaches for β and $\mathbf{\Theta}$ (or equivalently α) have been derived to enable full-diversity and full-rate in [1]. The LCF coded symbols $\{\mathbf{u}_g\}_{g=1}^{N_t}$ then go through an LST mapper, and are transmitted through N_t antennas as follows:

$$\begin{bmatrix} u_1(1) & u_{N_t}(2) & \ldots & u_2(N_t) \\ u_2(1) & u_1(2) & \ldots & u_3(N_t) \\ \vdots & \vdots & \ldots & \vdots \\ u_{N_t}(1) & u_{N_t-1}(2) & \ldots & u_1 N_t \end{bmatrix}, \begin{matrix} \rightarrow & \text{time} \\ \downarrow & \text{space} \end{matrix} \tag{3}$$

where $u_g(k)$ denotes the kth entry of vector $\mathbf{u}_g$. Let ^{T} denote transposition and $\mathbf{s} := [\mathbf{s}_1^T, \ldots, \mathbf{s}_{N_t}^T]^T$ denote one FDFR block. With $\otimes$ standing for Kronecker's product, $\boldsymbol{\theta}_i^T$ denoting the ith row of $\mathbf{\Theta}$, and by defining the permutation matrix $\mathbf{P}_i$ and the diagonal matrix $\mathbf{D}_\beta$, respectively, as:

$$\mathbf{P}_i := \begin{bmatrix} \mathbf{0} & \mathbf{I}_{i-1} \\ \mathbf{I}_{N_t-i+1} & \mathbf{0} \end{bmatrix} \quad \text{and} \quad \mathbf{D}_\beta := \mathrm{diag}[1, \beta, \ldots, \beta^{N_t-1}],$$

we obtain the equivalent FDFR encoder for the entire block as

$$\mathbf{\Phi} := \begin{bmatrix} (\mathbf{P}_1 \mathbf{D}_\beta) \otimes \boldsymbol{\theta}_1^T \\ \vdots \\ (\mathbf{P}_{N_t} \mathbf{D}_\beta) \otimes \boldsymbol{\theta}_{N_t}^T \end{bmatrix}. \tag{4}$$

We use $\mathbf{H}$ to denote the $N_r \times N_t$ MIMO channel coefficient matrix between transmit and receive antennas, which is assumed to be constant over each FDFR block. Thus, the channel matrix for the N_t transmitted vectors can be written as:

$$\boldsymbol{\mathcal{H}} := \mathbf{I}_{N_t} \otimes \mathbf{H}. \tag{5}$$

Let $\mathbf{y}_k$ denote the kth $N_r \times 1$ received vector, $\mathbf{y} := [\mathbf{y}_1^T, \ldots, \mathbf{y}_{N_t}^T]^T$, $\mathbf{n}_k$ denote the kth $N_t \times 1$ noise vector, and $\mathbf{n} := [\mathbf{n}_1^T, \ldots, \mathbf{n}_{N_t}^T]^T$. The input-output relationship is then [1]:

$$\mathbf{y} = \boldsymbol{\mathcal{H}}\mathbf{\Phi}\mathbf{s} + \mathbf{n} = \mathbf{H}_{eq}\mathbf{s} + \mathbf{n}, \tag{6}$$

where the equivalent channel matrix for the entire FDFR block is $\mathbf{H}_{eq} = \boldsymbol{\mathcal{H}}\mathbf{\Phi}$.

At the receiver end, iterative decoding is carried out to achieve an overall near-ML performance. Two modules, indexed by subscripts $_1$ and $_2$, perform the soft decoding for FDFR and ECC, respectively. Extrinsic information about $\mathbf{c}$ denoted as $\boldsymbol{\lambda}_E$ from one decoding module is interleavered or deinterleavered to yield *a priori* information about $\mathbf{c}$ denoted as $\boldsymbol{\lambda}_A$ for the other module. After a certain number of iterations or after a certain bit error rate (BER) is achieved, hard decision $\hat{\mathbf{b}}$ is made based on the *posteriori* information about $\mathbf{b}$ denoted as $\boldsymbol{\lambda}_{D2}$ from the ECC decoding module.

Inside each module, the optimal maximum *a posteriori* (MAP) decoder, whether it operates over the Galois Field (GF) or over the real/complex field (RCF), requires complexity exponential to the block size, or the constellation size, in general. Several near-optimal algorithms with polynomial complexity have been developed for the GF and the RCF cases, respectively. Those for decoding over GF are pretty standard when CC or TC are used. We adopt the so called log-MAP algorithm to decode CC and TC [5] in this paper. We use the near-optimal SHD-SD schemes developed in [3] to decode FDFR for QPSK signalling. Other constellations will be considered later.

Compared with coded V-BLAST, the system model of which is obtained by replacing the entire FDFR design module with a serial to parallel converter in Figure 1, both systems have the same transfer rate $R_c \times N_t$ symbols per channel use, for the same ECC rate R_c. However, the performance analysis presented next will show that the diversity order enabled by coded FDFR is N_t times that enabled by coded V-BLAST. In this paper, we focus on the performance comparison between the coded FDFR and the coded V-BLAST systems. So we use the same SHD-SD 2 [3] to decode the MIMO channels in both systems. Notice that the equivalent channel matrix $\mathbf{H}_{eq}$ is an $N_t^2 \times N_r^2$ complex matrix, which implies a considerable increase in decoding complexity relative to V-BLAST with block size N_t in the same antenna setup, if the same decoding scheme is used for both. A lower complexity decoder for FDFR is postponed for the future research.

III. Performance analysis

We here resort to the pairwise error probability (PEP) analysis to analyze the performance of coded FDFR. Consider two different information bit sequences $\mathbf{b}^{\langle 1 \rangle}$ and $\mathbf{b}^{\langle 2 \rangle}$. They yield two codewords $\mathbf{c}^{\langle 1 \rangle}$ and $\mathbf{c}^{\langle 2 \rangle}$ after ECC. These two codewords differ from each other in W positions. Under the assumption that the interleaver Π is random and sufficiently long, after constellation mapping, the two symbol sequences $\mathbf{s}^{\langle 1 \rangle}$ and $\mathbf{s}^{\langle 2 \rangle}$ still have W different symbols, and the positions where they differ are spread far away from each other. Therefore, in any FDFR block the vectors $\mathbf{s}(k)^{\langle 1 \rangle}$ and $\mathbf{s}(k)^{\langle 2 \rangle}$ differ in at most one symbol, where $k \in [1, K]$ indexes the FDFR block, and K is the number of FDFR blocks.

After LCF coding, LST mapping, and the physical channel $\mathbf{H}(k)$, the equivalent channel matrix for the kth FDFR block is $\mathbf{H}_{eq}(k)$. The resulting symbol vectors are $\{\mathbf{z}(k)^{\langle 1 \rangle} = \mathbf{H}_{eq}(k)\mathbf{s}(k)^{\langle 1 \rangle}\}_{k=1}^{K}$ and $\{\mathbf{z}(k)^{\langle 2 \rangle} = \mathbf{H}_{eq}(k)\mathbf{s}(k)^{\langle 2 \rangle}\}_{k=1}^{K}$. Among K blocks, only W of them are different. Without causing confusion, we will use $\{\mathbf{z}(w)^{\langle 1 \rangle}\}_{w=1}^{W}$ and $\{\mathbf{z}(w)^{\langle 2 \rangle}\}_{w=1}^{W}$ to denote them. When $\mathbf{s}(w)^{\langle 1 \rangle}$ and $\mathbf{s}(w)^{\langle 2 \rangle}$ are different in the mth symbol, the Euclidean distance between $\mathbf{z}(w)^{\langle 1 \rangle}$ and $\mathbf{z}(w)^{\langle 2 \rangle}$

is:

$$||\mathbf{z}(w)^{\langle 1\rangle} - \mathbf{z}(w)^{\langle 2\rangle}||^2 = ||\mathbf{h}_{eq,m}(w)||^2 |\Delta s_m(w)|^2, \quad (7)$$

where $\mathbf{h}_{eq,m}(w)$ is the mth column of the equivalent channel matrix $\mathbf{H}_{eq}(w)$, and $|\Delta s_m(w)|^2$ is the Euclidean distance between the two different symbols $s_m(w)^{\langle 1\rangle}$ and $s_m(w)^{\langle 2\rangle}$. With δ^2 standing for the minimum Euclidean distance between two symbols, we have that

$$|\Delta s_m(w)|^2 \geq \delta^2. \quad (8)$$

Since $\mathbf{H}_{eq} = \boldsymbol{\mathcal{H}}\boldsymbol{\Phi}$, by the definitions of $\boldsymbol{\mathcal{H}}$ in (5) and $\boldsymbol{\Phi}$ in (4), when the mth symbol is in the gth FDFR sub-block, then

$$||\mathbf{h}_{eq,m}(w)||^2 = ||\boldsymbol{\mathcal{H}}(w)\boldsymbol{\phi}_m||^2 = \sum_{i=1}^{N_r}\sum_{j=1}^{N_t} |h_{i,j}(w)|^2 |\theta_{g,(j,m)}|^2$$

$$= (1/N_t)\sum_{i=1}^{N_r}\sum_{j=1}^{N_t} |h_{i,j}(w)|^2, \quad (9)$$

where $\boldsymbol{\phi}_m$ is the mth column of $\boldsymbol{\Phi}$, $h_{i,j}(w)$ is the (i,j)th entry of $\mathbf{H}(w)$, and $\theta_{g,(j,m)}$ is the $(j, m \bmod N_t)$th entry of $\boldsymbol{\Theta}_g$. Eq. (9) is true because all entries of $\boldsymbol{\Theta}_g$ have equal norm $1/\sqrt{N_t}$.

From (7), (8) and (9), the overall Euclidean distance of this two sequences obeys

$$d_{1,2}^2 = \sum_{w=1}^{W} ||\mathbf{z}_w^{\langle 1\rangle} - \mathbf{z}_w^{\langle 2\rangle}||^2 \geq \delta^2/N_t \sum_{w=1}^{W}\sum_{i=1}^{N_r}\sum_{j=1}^{N_t} |h_{r,j}(w)|^2.$$

The pairwise error probability for a given channel realization, $P_{1,2|H} := P(\mathbf{c}^{\langle 1\rangle} \rightarrow \mathbf{c}^{\langle 2\rangle} | \{\mathbf{H}_k\})$, can be upper bounded as:

$$P_{1,2|H} \leq Q\left(\sqrt{\frac{\delta^2/N_t \sum_{w=1}^{W}\sum_{i=1}^{N_r}\sum_{j=1}^{N_t} |h_{r,j}(w)|^2}{2N_0}}\right),$$

where $Q(x) := \int_x^\infty (1/\sqrt{2\pi})\exp(-\alpha^2/2)d\alpha$. Using the chernoff bound $Q(x) \leq (1/2)\exp(-x^2/2)$ and averaging over the complex Gaussian distribution of the h's, we obtain

$$P_{1,2} \leq 1/2\left(1 + \frac{\delta^2}{4N_tN_0}\right)^{-WN_tN_r} \quad (10)$$

Eq. (10) shows that a diversity order of WN_tN_r is achieved for the PEP. After applying the union bound to all error events, we can further show that a diversity order dN_tN_r is achieved for the BER, where d is the minimum Hamming distance of the block ECC, or the free distance of the CC. The detailed proof is omitted due to space limitation. The diversity order of coded V-BLAST can be similarly shown to be dN_r. Coded FDFR thus enables a diversity order N_t times higher than coded V-BLAST.

IV. Simulations

We carried out simulations with different ECC's for QPSK signalling. We here compare the BER performance of the coded V-BLAST and FDFR systems using the soft-to-hard sphere decoder (SHD-SD2) of [3]. The interleaver size is chosen to be 2^{10}. The channels are fast i.i.d. flat fading, remaining constant within an FDFR block but independent between FDFR blocks. In each figure, the curves with the same marker are BER curves for the same system (either coded V-BLAST or coded FDFR) at different iterations.

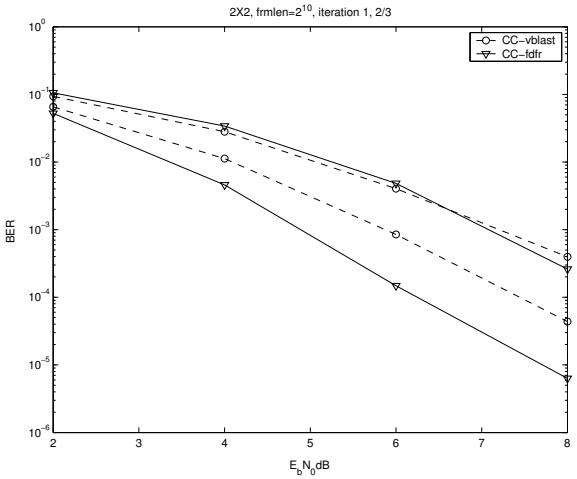

Fig. 2. 1/2 convolutional codes with FDFR v.s. 1/2 convolutional codes with V-BLAST in 2×2 setup

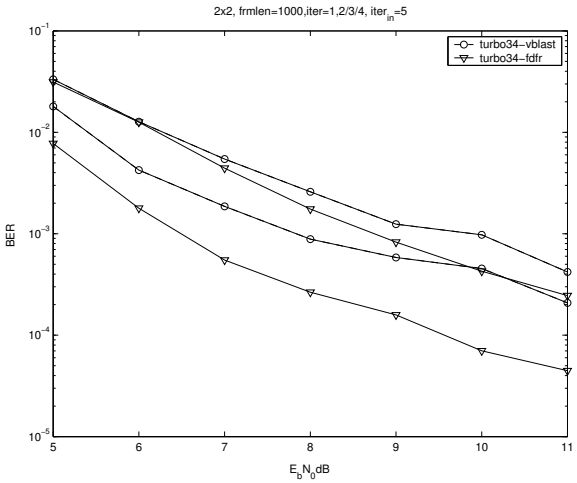

Fig. 3. 3/4 turbo codes with FDFR v.s. 3/4 turbo codes with V-BLAST in 2×2 setup

Simulation 1: Figures 2 and 3 depict BER performance comparison between coded V-BLAST and coded FDFR, when relatively weak codes (CC and high rate TC) are used as ECC modules in a 2×2 antenna setup. BER curves with two iterations are shown, because the gain after the 2rd iteration for both systems was negligible. We use rate 1/2 CC with memory 2, feedback polynomial $G_r(D) = 1+D+D^2$, and feedforward polynomial $G(D) = 1 + D^2$. About 1.5dB gain at BER=10^{-4} is offered by the FDFR design when CC is used. We also use rate 3/4 parallel concatenated convolutional codes (PCCC) in Figure 3, composed of two CC modules parameterized as above. The puncturing patten used retained all systematic bits and took one bit every 6 bits from each coded stream. Five iterations are performed inside the decoding module for rate 3/4 turbo codes. Two outer iterations are performed between the two decoding

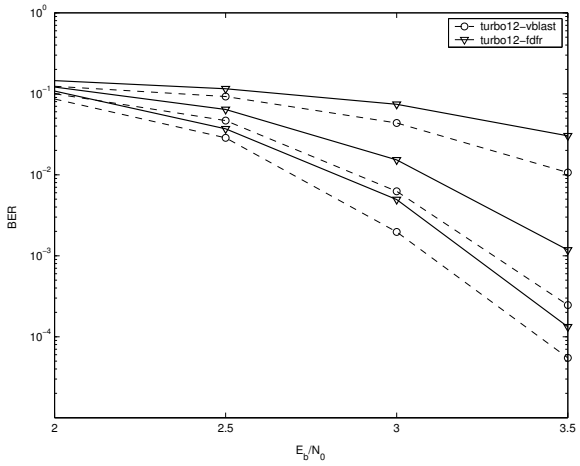

Fig. 4. 1/2 turbo codes with FDFR v.s. 1/2 turbo codes with V-BLAST in 2×2 setup

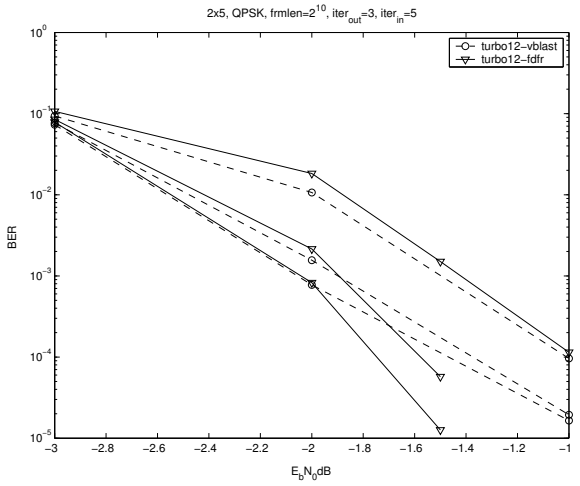

Fig. 5. 1/2 turbo codes with FDFR v.s. 1/2 turbo codes with V-BLAST in 2×5 setup

modules. Figures 3 shows the performance comparison for rate 3/4 turbo codes in a 2×2 setup. In this case, coded FDFR outperforms coded V-BLAST by about 2dB.

Simulation 2: In this simulation, we use a rate 1/2 PCCC constructed as with the rate $3/4$ PCCC except for the puncturing patten. Here we keep all the systematic bits and every other bit from each coded stream. Figure 4 depicts the comparison in a 2×2 setup with three outer iterations. Five iterations are performed inside the decoding module for rate 1/2 turbo codes. We observe that the coded V-BLAST system outperforms the coded FDFR system about 0.1dB. It is reasonable that when such a strong code as 1/2 TC is used with $N_r = N_t$, no performance improvement with FDFR is obtained. At low SNR, the performance improvement is brought mainly through the coding gain. Since the FDFR design is non-redundant, FDFR has no positive effect at low SNR. FDFR enhances the performance by providing extra diversity, the effect of which is notable at high SNR. However, when we use strong codes such as a rate $1/2$ TC, at high SNR the diversity gains are already high (i.e., the slope of the BER curve is already very steep). Therefore, the extra diversity provided by FDFR is not useful is this case. The reason coded FDFR yields to coded V-BLAST might be the fact that as the MIMO block size increases the decoding becomes less accurate. Figure 5 shows the same comparison in a 2×5 setup. By increasing N_r, both coded FDFR and coded V-BLAST benefit from the extra energy collected and the extra diversity provided by N_r receive antennas. But the turbo gain between iterations becomes smaller. We further observe that in the 2×5 case, even the coded LST system with rate 1/2 TC can benefit from the FDFR design by about 0.5dB over the coded V-BLAST system.

Remark: From Figures 2 to 5, we can observe an evident iterative gain between iterations for both coded V-BLAST and coded FDFR. This observation is different from the conclusion in [6] that no improvement is brought by performing outer iterations between the space-time decoding module and the decoding module for outer code. This is because the assertion in [6] has been established only for space-time orthogonal designs, where the equivalent channel is diagonal and thus the *a priori* information from other symbols provides no extra information for the current symbol. This clearly does not hold for FDFR and V-BLAST.

V. Conclusions

In this paper we investigated the performance of a coded full-diversity full-rate (FDFR) system. For any number of N_t transmit and N_r receive antennas and rate R_c error-control coding, high rate ($R_c N_t$ symbols per channel use) and high diversity order (dN_tN_r) are achieved. Compared with its coded V-BLAST counterpart, coded FDFR improves performance without sacrificing rate. The price paid is increase in complexity. How to softly decode FDFR with low complexity is an issue worth pursuing.

Acknowledgement: The work in this paper was supported by the ARL/CTA Grant No. DAAD 19-01-2-0011.

References

[1] X. Ma and G. B. Giannakis, "Full-diversity full-rate complex-field space-time coding," *IEEE Trans. on Signal Processing*, vol. 51, pp. 2917–2930, Nov. 2003.

[2] R. Wang, Z. Wang, and G. B. Giannakis, "Combining Galois with complex field coding for space-time communications," *European Telecommunications Transactions*, vol. 14, no. 1, pp. 25–36, Jan./Feb. 2003.

[3] R. Wang and G.B. Giannakis, "Approaching MIMO Channel capacity with reduced-complexity soft sphere decoding," *IEEE Trans. on Communications*, July 2003 (submitted).

[4] B. M. Hochwald and S. ten Brink, "Achieving near-capacity on a multiple-antenna channel," *IEEE Trans. on Communications*, vol. 51, no. 3, pp. 389–399, Mar. 2003.

[5] P. Robertson, E. Villebrun, and P. Hoeher, "A comparison of optimal and suboptimal MAP decoding algorithms operating in the log domain," in *Proc. Intl. Conf. on Communications*, Seattle, Washington, June 1995, pp. 1009–1013.

[6] G. Bauch, "Concatenation of space-time block codes and turbo-TCM," in *IEEE International Conference on Communications*, Vancouver, Canada, 6-10 June 1999, vol. 2, pp. 1202–1206.